Industrial Chemistry & Materials

ROYAL SOCIETY OF CHEMISTRY

REVIEW

View Article Online
View Journal | View Issue

Cite this: *Ind. Chem. Mater.*, 2023, **1**, 79

Recent advances in the detection and removal of heavy metal ions using functionalized layered double hydroxides: a review

Wencai Liu,[a] Yang Liu,[a] Zhiqin Yuan *[a] and Chao Lu *[ab]

Heavy metal pollution is one of the most severe environmental problems, possessing high ecotoxicity and health risk. Therefore, it is important to develop effective methods and corresponding materials for the detection and removal of heavy metals. Recent studies reveal the great potential of layered double hydroxides (LDHs) in detecting and removing heavy metals owing to their designable structure and tunable surface composition. In this review, we majorly discuss the recently adopted detection and removal of heavy metal ions based on LDHs. This review starts with an introduction of the structural characteristics and functionalization of LDHs. Then, the sensing tactics and mechanisms are introduced regarding LDH-based heavy metal ion detection. Based on the type of interaction, the removal of heavy metal ions with LDHs is summarized into two categories: reversible adsorption and irreversible mineralization. This review ends with a discussion on the challenges and future trends of LDH-based detectors and adsorbents for heavy metal ions.

Received 2nd September 2022,
Accepted 25th October 2022

DOI: 10.1039/d2im00024e

rsc.li/icm

Keywords: Heavy metal ion; Layered doubled hydroxide; Detection; Removal.

1 Introduction

As one of the most severe environmental problems, heavy metal pollution causes health risks and is difficult to treat.[1] Even at the ppb level, some heavy metals are still harmful due to their strong binding affinity toward N, O, and S atoms of biomolecules, which inhibits biological functions and interrupts physiological processes.[2] For example, the catalytic activity of some enzymes is dramatically inhibited after Hg^{2+} or Cu^{2+} binding, which is known as heavy metal poisoning. Excess intake of heavy metals also leads to a variety of diseases, such as Alzheimer's disease, Parkinson's disease and amyotrophic lateral sclerosis.[3,4] In addition, heavy metals show high stability in many environments in comparison to organic compounds.[5] As a consequence, the detection and removal of environmental heavy metals is significant to ecological security.

[a] *State Key Laboratory of Chemical Resource Engineering, College of Chemistry, Beijing University of Chemical Technology, Beijing 100029, China. E-mail: yuanzq@mail.buct.edu.cn, luchao@mail.buct.edu.cn*
[b] *Green Catalysis Center, College of Chemistry, Zhengzhou University, Zhengzhou 450001, China*

Wencai Liu

Wencai Liu received her B.S. degree in chemistry from Hebei North University in 2020. She is currently a master student at Beijing University of Chemical Technology, Beijing, China. She is engaged in the preparation and characterization of layered double hydroxides and their applications in sensing.

Yang Liu

Yang Liu received his B.S. degree in chemistry from Beijing University of Chemical Technology in 2020. He is currently a master student at Beijing University of Chemical Technology, Beijing, China. He is engaged in the design, synthesis and application of small molecule probes and organic–inorganic hybrid materials.

Toward this goal, considerable effort has been devoted to the development of heavy metal sensors and adsorbents using organic and inorganic materials with the integration of various techniques.[6–10] For instance, rhodamine and coumarin derivatives have been widely explored as fluorescent probes for various heavy metal ions.[11] Using hyperbranched polyethyleneimine-capped silver nanocluster as fluorescence probe, Yuan *et al.* achieved sensitive Cu^{2+} detection with a limit of detection (LOD) of 10 nM.[12] Metal–organic framework-based materials have been applied for the adsorption and removal of heavy metal ions.[13–16] Recently, layered double hydroxides (LDHs) with large specific surface area and tunable composition/structure have shown great potential in designing effective heavy metal detectors and adsorbents.[17–21] Their easy preparation, low-cost, and exchangeable interlayer anions make LDHs attractive in removing heavy metal ions in comparison to other materials.[22,23] For example, Li *et al.* reported the selective and electrochemical detection of Pb^{2+} with Fe/Mg/Ni ternary LDHs.[24] Using CaAl-LDH as an adsorbent, Kong *et al.* explored efficient Cd^{2+} removal in aqueous media with a high adsorption capacity of 592 mg g^{-1}.[25] In consideration of the adjustable layer composition and interlayer anions, appropriately functionalized LDHs can be applied for productive heavy metal ion detection and removal by integrating proper monitoring. We have witnessed recent advances in LDH-based probes and adsorbents in rapid and efficient heavy metal ion detection and removal due to their improved sensitivity, selectivity, and stability.

Despite the report of few excellent review articles on LDH-based adsorbent exploration in the past few years,[26–29] summarizing some of the most recent developments in both heavy metal ion detection and removal will help junior researchers to understand the fundamental principles and to select proper strategies for constructing expected LDH probes and adsorbents. In this review, the structure and functionalization of LDHs are first introduced. Then, recent advances in LDH-based analysis systems for heavy metal ions (*e.g.*, Cd^{2+}, Pb^{2+}, and Cu^{2+}) are summarized in four aspects: colorimetric assays, fluorimetric assays, electrochemical assays, and atomic absorption spectrometry (National standard method). Meanwhile, the sensing mechanisms or approaches of analyte-induced signal changes are discussed. Recent studies showed that ion exchange-induced mineralization is more effective to realize ultrastable adsorption of heavy metal ions. Thus, regarding the LDH-based nanosorbents, the removal of heavy metal ions is classified into reversible adsorption and irreversible mineralization for the first time. In consideration of the page limit, only few examples are selected in each described section. Finally, this review ends with the discussion of current challenges and future prospects of LDHs for sensing and mineralization applications.

2 Structure and functionalization of LDHs

LDHs are a large class of two-dimensional materials with positively charged brucite-like metal hydroxide layers and charge-balancing intercalated anions, as shown in Fig. 1a.[30] The metal ions of outer layers possess unsaturated coordination, which requires auxiliary chelation with hydroxyl groups. The abundance of surface hydroxyl groups usually makes LDH suspensions alkaline. The structural formula of the LDH can be described as $[M^{2+}_{1-x}N^{3+}_{x}(OH)_2]^{x+}(A^-)_{x/n}\cdot mH_2O$, where M^{2+} and N^{3+} stand for divalent and trivalent metal cations, and A^- represents interlayer anions. In many cases, the K_{sp} values of LDHs are much smaller than that of the corresponding $M(OH)_2$ and $N(OH)_3$ due to the ultrastable steric configuration of the layer structure and high coordination number of metal cations. As a result, the co-existence of M^{2+}, N^{3+} and OH^- has a tendency

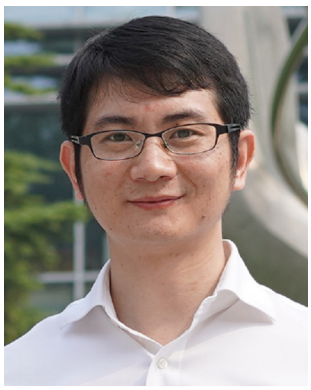

Zhiqin Yuan

Zhiqin Yuan is currently an Associate Professor at the College of Chemistry, Beijing University of Chemical Technology. He obtained his PhD from the College of Chemistry and Chemical Engineering, Hunan University, in 2013 with Dr Yan He and Dr Edward S. Yeung. His research interests are focused on synthesis and analytical application of metal nanoparticles and nanoclusters, carbon quantum dots, and layered nanomaterials.

Chao Lu

Chao Lu received his Ph.D. degree in Materials Science from Chinese Academy of Sciences in 2004. He is currently a full professor of Green Catalysis Center, College of Chemistry, Zhengzhou University. In 2011, he was selected to participate in the 'New Century Outstanding Talent' scheme of the Ministry of Education. His research interests are focused on the synthesis and characterization of nanostructured materials, nanosensors, and chemiluminescence. He is responsible for national and international research projects and has published more than 100 papers.

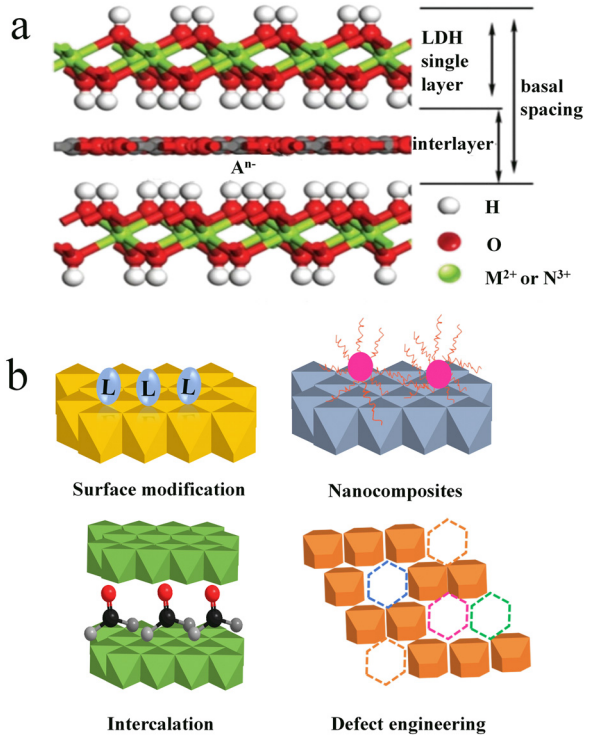

Fig. 1 (a) Schematic of the LDH structure. Reprinted with permission from ref. 30. Copyright 2020, Royal Society of Chemistry. (b) Schematic illustration of four ways of LDH functionalization.

to form MN-LDHs rather than $M(OH)_2$ and $N(OH)_3$. So far, many synthetic procedures have been explored for the preparation of LDHs, including coprecipitation, hydrothermal synthesis, ion exchange, structure reconstruction, and so on.[31]

Similar to other two-dimensional materials, LDHs also show large specific surface areas and high adsorption capability toward ions and molecules.[32,33] And the adsorption performances of LDHs are related to the chemical composition, structure, shape and size of inorganic metal hydroxide layers and also the interlayer gallery anions. In addition, the chemical reactivity of LDHs connects with the thickness of the cationic layer, which is controlled by the chemical identity of the metal ions and the size of intercalated anions. Interestingly, the chemical composition of metal hydroxide layers, as well as the interlayer anions can be precisely controlled.[34]

Despite the easy preparation of LDHs with low costs, the finite functional groups and simple structural components limit the applications of original LDHs in sensing and adsorption. Therefore, it is important to enhance the performances or create new functions of LDHs by importing functional groups or structural components. To increase the functional groups, two pathways are considered. One is to introduce functional molecules or compounds; the other is to break the integrated structure of LDHs. The former fixes functional molecules on the LDH surface or into the interlayer, while the latter creates defects on LDHs. Functionalization of LDHs can be achieved simply by surface modification with organic molecules containing functional groups. The increased functional groups promote the binding affinity for various heavy metal ions. By changing organic molecules into nanomaterials, the resulting nanomaterial-LDH hybrids contribute combined functions toward different applications, such as adsorption, magnetic separation, catalysis, *etc.* In addition, the change of interlayer anions into inorganic and organic anions, coordination compounds, polyoxometalates, and biomolecules is also an effective way to construct function-designable LDHs.[35] Moreover, substituting metal cations of hydroxide layers with various divalent and trivalent metal ions also benefits the binding of various small molecules or polymers.[36] Meanwhile, the substitution might produce defects into the LDH layer, which is regulated by changing the dosage of the metal source.[30,37] As referred in Chen's report, oxygen defects into the LDH layer enhance the ion exchange between the LDH layer and heavy metal ions.[38] Besides metal substitution, plasma treatment is also an effective means to generate defects into the LDH layer. In a word, the functionalization of LDHs could be realized by surface modification, nanocomposites, intercalation science and defect engineering (Fig. 1b).

3 Detection of heavy metal ions

As mentioned above, heavy metal pollution causes severe environmental problems, and the development of sensitive and selective detection methods is attracting growing attention in recent years. The rich hydroxyl group on the surface, as well as the various interlayer anions, makes LDHs a good candidate to construct efficient heavy metal ion sensors by integrating proper techniques. Accordingly, for the detection of heavy metal ions, LDH-based sensing systems have been proposed according to four categories: colorimetric assays, fluorimetric assays, electrochemical assays and atomic absorption spectrometry.

3.1 Colorimetric assays

Colorimetric detection methods are simple, fast and low-cost, and the surface group-metal interaction could be applied for the design of selective heavy metal ion sensors with colorimetric changes.[39–43] For example, cysteamine functionalized gold nanoparticles have been explored for colorimetric detection of Cu^{2+} through forming aggregates.[12] This is because the aggregation of gold nanoparticles alters surface plasmonic resonance and leads to color changes of the colloid solution from red to blue. However, neither dispersive nor aggregated LDHs show a visible colour as in gold nanoparticle systems. As a result, chromophores are introduced into LDH-based sensing systems to produce a colour change.

The metal hexacyanoferrates show unique colours, which has been applied to metal ion identification. On the basis of this character, Wang *et al.* developed a colorimetric Fe^{3+} and Cu^{2+} sensing system using $Fe(CN)_6^{4-}$ anion interlayered MgAl-LDH modified test strips (Fig. 2a).[44] Without the addition of heavy metal ions, the LDH control displayed the

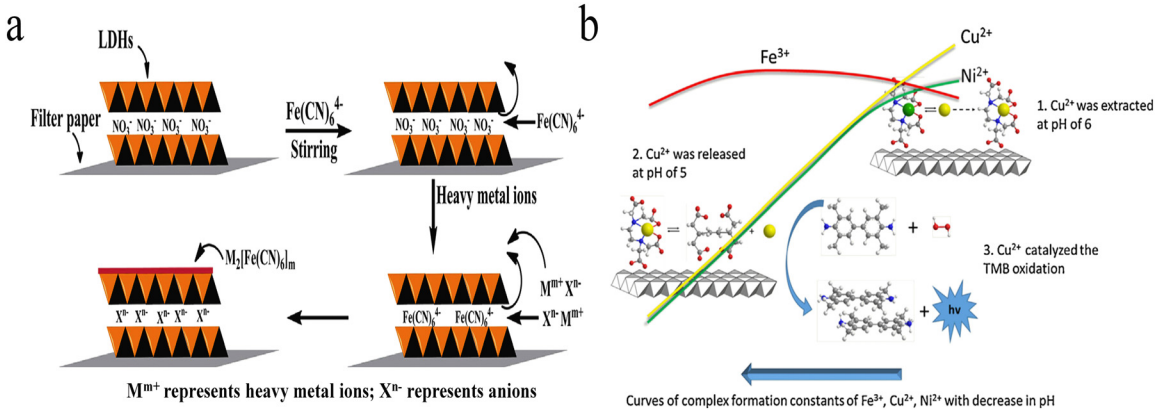

Fig. 2 (a) Illustration of the concept for the formation of $Fe(CN)_6^{4-}$ anion-interlayered MgAl-LDH-modified test strips and the detection of heavy metal ions. Reprinted with permission from ref. 44. Copyright 2016, Elsevier. (b) Schematic of the selective extraction–release–catalysis detection process. Reprinted with permission from ref. 45. Copyright 2015, Elsevier.

natural colour of filter paper. Interestingly, a dramatic colour change was observed within 30 s upon adding Fe^{3+} or Cu^{2+}. Blue colour appeared after the addition of Fe^{3+}, which is due to the formation of Prussian blue, while the introduction of Cu^{2+} led to the formation of copper hexacyanoferrate precipitates, resulting in the appearance of reddish brown colour. With naked-eye observation, 50 μM Fe^{3+} or 10 μM Cu^{2+} were detectable.

In addition to forming colourful precipitates, few transition heavy metal ions possess strong catalytic activity toward H_2O_2, called Fenton or Fenton-like reaction, which generates reactive oxygen species and leads to the oxidation of chromophore precursors. Based on this property, Tang *et al.* reported a colorimetric system toward Cu^{2+} and Fe^{3+}.[45] In their work, ethylenediaminetetraacetic acid (EDTA)–nickel ion (Ni^{2+}) chelates were first intercalated into LDHs by co-precipitation reaction. The chelated Ni^{2+} could be replaced by Cu^{2+} due to the high complex formation constant of EDTA–Cu^{2+}. The Ni^{2+}–Cu^{2+} exchange reaction was effective under pH 6.0, which extracts soluble Cu^{2+} to the LDH surface. As is known, the acidic effect coefficient of EDTA is oppositely proportional to the solution pH. That is, the lower the pH, the stronger the acidic effect coefficient. Large acidic effect coefficient results in low complex formation constant and the release of chelated metal ions. When the solution pH was adjusted to 5, the chelated Cu^{2+} was released from the LDH surface and catalysed the oxidation of 3,3,5,5-tetramethylbenzidine (TMB) in the presence of H_2O_2 through Fenton-like reaction, which produces a chromogenic compound with high absorption coefficients (Fig. 2b). The blue colour of oxidized TMB allowed for the colorimetric detection of Cu^{2+} in the concentration range from 0.05 to 100 μM, with a LOD of 10 nM.

They also found that aniline catalytic polymerization was realized in the presence of Cu^{2+} or Fe^{3+}.[46] With the combination of metal ion exchange and aniline catalytic polymerization, sensitive detection of Cu^{2+} or Fe^{3+} was achieved using LDHs as the support. The enrichment of Cu^{2+} and Fe^{3+} was conducted at pH 6.5 and 4.5, respectively. Through the pH adjustment, free Cu^{2+} or Fe^{3+} was released from the complex and catalysed the polymerization of aniline. The strong hydrolysis of Fe^{3+} required the enrichment with high acidity. However, in a weakly acidic or neutral environment, $Fe(OH)_3$ was easily formed. In this case, the EDTA–Fe^{3+} complex formation constant at pH 6.5 was smaller than that of pH 4.5. In contrast, EDTA–Cu^{2+} complex formation constant increased with the increasing pH from 4.5 to 6.5. Taken together, the enrichment pHs for Cu^{2+} and Fe^{3+} were 6.5 and 4.5, while the release pHs were 4.5 and 6.5, respectively. According to the absorption spectra of polymeric aniline, the detection of Cu^{2+} and Fe^{3+} was performed at 0.1 and 1 nM, respectively.

3.2 Fluorimetric assays

Fluorimetry shows the advantages of low background, high sensitivity and strong interference rejection, and has attracted wide research interest in the past decades.[47,48] Ligand functionalized nanomaterials (*e.g.*, gold nanoclusters and semiconducting quantum dots) have been applied in the detection of heavy metal ions, including Pb^{2+}, Hg^{2+}, Cu^{2+}, and so on.[49,50] Since the autofluorescence of LDHs is generally ignorable, fluorescent materials are usually introduced to construct LDH-based fluorimetric heavy metal ion detection systems. Through the fluorescence variation, these systems can be classified into two categories: fluorescence turn-off system and fluorescence turn-on system.[51,52]

For many heavy metals, the paramagnetic atomic orbital easily causes the fluorescence quenching of adjacent fluorophores, making the fluorescence quenching probes commonly used in the detection of heavy metal ions. To light up LDHs, fluorescent organic or inorganic materials are used.[52] In general, ultrathin films with bright emission were fabricated through layer-by-layer assembly of LDHs and fluorophores.[53] For example, Shi *et al.* proposed a Cd^{2+} probe based on ZnAl-LDH nanosheets and 2,20-azino-bis(3-ethylbenzothiazoline-6-sulfonate) (ABTS).[54] As shown in Fig. 3a, fluorescent ultrathin films through layer-by-layer deposition were first constructed. The addition of Cd^{2+}

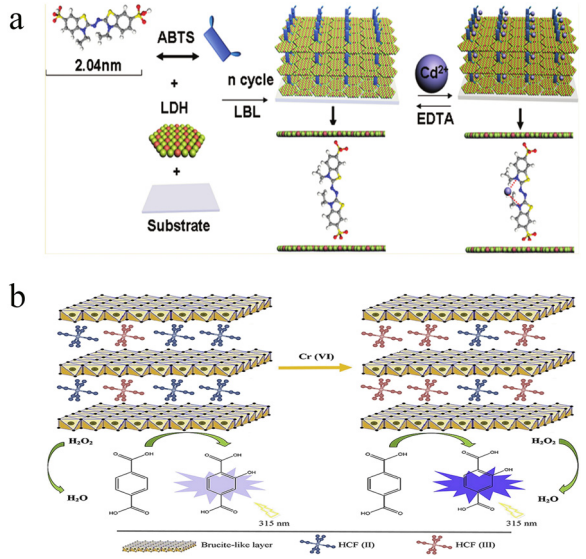

Fig. 3 (a) Schematic of fluorimetric Cd^{2+} detection using an ultrathin film from ZnAl-LDH nanosheets and ABTS. Reprinted with permission from ref. 54. Copyright 2011, American Chemical Society. (b) Schematic illustration of fluorescence turn-on Cr(VI) based on $Fe(CN)_6^{4-}$-intercalated NiAl-LDHs and TA. Reprinted with permission from ref. 58. Copyright 2020, Elsevier.

caused the distinct fluorescence quenching of ABTS, and the intensity at 435 nm can be used for the monitoring of Cd^{2+} concentration, with a LOD of 9.5 nM. Such a Cd^{2+}-induced fluorescence inhibition can be recovered by adding EDTA. This is because the complex formation constant of EDTA–Cd^{2+} is larger than that of ABTS–Cd^{2+}. This character allowed for the cyclic Cd^{2+} detection. By replacing ABTS with pyrenetetrasulfonate (PTS), they established a Cu^{2+} detection platform with a similar tactic.[55] The strong PTS-Cu^{2+} binding affinity ruled out the interference from other metal ions, such as Pb^{2+}, Co^{2+} and Ni^{2+}.

In addition to organic fluorophores, fluorescent inorganic nanomaterials were also applied for the fabrication of fluorimetric sensors. For instance, Mn-doped ZnS (Mn-ZnS) semiconducting quantum dots and MgAl-LDHs were used to establish a fluorimetric sensing platform toward Pb^{2+}, Cr^{3+} and Hg^{2+}.[56] The glutathione stabilized Mn-ZnS quantum dots adsorbed onto the MgAl-LDH surface *via* electrostatic attraction, yielding fluorescent nanocomposites. Under an optimal quantum dot/LDH ratio, the fluorescence was greatly enhanced, partially due to the inhibited aggregation of Mn-ZnS quantum dots by MgAl-LDH supports. The fluorescence quenching of Mn-ZnS quantum dots was assigned to the surface cation exchange reaction, which breaks the energy gap. Interestingly, the fluorescence intensities decreased with similar trends upon adding Pb^{2+}, Cr^{3+} and Hg^{2+}. The comparable quenching efficiencies were attributed to the similar K_{sp} values of PbS ($10^{-27.1}$), HgS ($10^{-24.5}$) and Cr_2S_3 (insoluble in water) and relatively high K_{sp} value of MnS ($10^{-12.6}$). The low K_{sp} drove the rapid surface cation exchange reaction and caused dramatic fluorescence suppression.

Fluorescent Eu-MOF has also been explored as the reporter; Yang *et al.* proposed a Fe^{3+} turn-off sensor by integrating Eu-MOF and NiAl-LDHs.[57] The outer layer of Eu-MOF acted as the fluorescence reporter, while the inner NiAl-LDHs functioned as the Fe^{3+} captor. The Fe^{3+}-induced fluorescence quenching was divided into two pathways: inner filter effect and electron transition. A moderate overlap between the absorption spectrum of Fe^{3+} solution and the excitation spectrum of Eu-MOF was observed, resulting in a visible inner filter effect. In addition, the Fe^{3+} possesses a $3d^5$ outer electronic structure with five half-filled orbitals, which facilitates the electron transfer from the conduction band of the Eu-MOF to the 3d orbital of Fe^{3+} and quenches the fluorescence. This system enabled sensitive Fe^{3+} detection with a LOD of 0.1 μM.

Apart from fluorescence quenching, fluorescence turn-on systems have also been reported. As indicated above, direct modification with fluorophores usually results in quenching behavior after addition of heavy metal ions. It is reported that LDHs show visible peroxidase-like activity, and this character has been widely applied in the development of sensitive chemiluminescence sensing systems. To avoid fluorescence quenching, a non-fluorescent precursor was first introduced; then, the production of a fluorescent product by catalytic reaction was applied. Amini *et al.* presented a fluorescence turn-on system toward Cr(VI) based on $Fe(CN)_6^{4-}$ intercalated NiAl-LDHs and terephthalic acid (TA).[58] The $Fe(CN)_6^{4-}$ intercalated NiAl-LDHs exhibited peroxidase-like activity towards the TA–H_2O_2 system, which produces a highly fluorescent product (Fig. 3b). Such a peroxidase-like activity was dramatically promoted by the introduction of Cr(VI), because of the oxidation of $Fe(CN)_6^{4-}$ and formation of $Fe(CN)_6^{3-}$. The $Fe(CN)_6^{4-}$ and $Fe(CN)_6^{3-}$ mixture undergoes conversion of Fe^{2+}/Fe^{3+}, which accelerates the electron transfer and enhances the catalytic reaction. As a result, the fluorescence intensity at 422 nm was proportional to the Cr(VI) concentration, and showed good linearity in the concentration range from 0.067 to 10 μM. With this proposed system, sensitive Cr(VI) detection was achieved with a LOD of 0.039 μM. The Cr(VI)-caused $Fe(CN)_6^{4-}$ oxidation and subsequent activity promotion was selective; other heavy metal ions didn't show a similar response.

Note that electron transition energy in certain metal atoms is characteristic, and the corresponding atomic emission can be used to identify metal species. With the combination of the X-ray fluorescence technique, fluorimetric heavy metal detection can be realized without the involvement of fluorescent reporters. For example, based on this mechanism, Zawisza *et al.* proposed a turn-on gold detection method using MgAl-LDH/graphene oxide nanocomposites.[51] High sorption efficiencies toward both gold nanoparticles and Au^{3+} were realized by the nanocomposites. Through X-ray fluorescence determination, sensitive gold identification was achieved with a LOD of 0.06 ng mL^{-1}.

3.3 Electrochemical assays

For most colorimetric and fluorimetric assays, only one heavy metal target can be detected in a single test to prevent the

interference. However, multiple heavy metal ions usually exist if pollution occurs. Therefore, the development of simple and effective approaches for achieving simultaneous detection of multiple heavy metal ions is appealing. As is well known, different heavy metals show diverse redox potentials, which provides the possibility to discriminate multiple heavy metal ions by electrochemical assays.[59] To realize potential-resolved heavy metal ion detection, electrodes with high electrochemical performances have been explored. For example, graphene-based electrodes with high electron transfer capability have been reported for the simultaneous detection of Cd^{2+}, Pb^{2+}, Cu^{2+}, and Hg^{2+}.[60,61]

Since LDHs show high affinity toward metal ions due to the surface hydroxyl groups and various interlayer anions, LDH-based electrochemical approaches were established for the detection of multiple heavy metal ions.[62] However, sole LDHs usually have poor conductivity and selectivity. To overcome this drawback, the combination of LDHs and other materials with high conductivity is reasonable to facilitate the electrochemical detection.[63] For instance, Ma *et al.* reported a sensitive electrochemical sensor based on a MgFe-LDH modified graphene electrode (Fig. 4a).[64] Through a one-step hydrothermal method, MgFe-LDHs were immobilized onto the surface of graphene nanosheets. The resulting hybrid materials displayed high specific surface areas and good electrical conductivity, which enhances the heavy metal ion binding and subsequent electron transfer. Based on the proposed functional electrode, simultaneous detection of Pb^{2+} and Cd^{2+} in aqueous media was achieved with good interference rejection. Using peak current as the signal, linear responses of Pb^{2+} (−0.55 V) and Cd^{2+} (−0.8 V) were found in the concentration range of 0.05–1.0 μM and 0.1–1.0 μM, respectively. The LODs towards Pb^{2+} and Cd^{2+} were 2.7 nM and 5.9 nM, respectively. The good average recoveries (96.25 to 107.5%) and small relative standard deviations (<4%) support the potential of practical heavy metal ion analysis in real water samples.

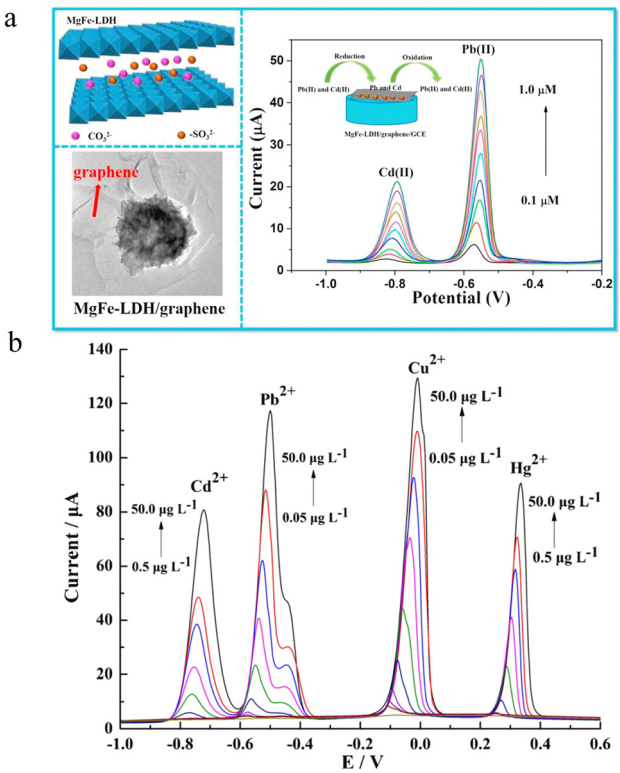

Fig. 4 (a) Schematic illustration of electrochemical Cd^{2+} and Pb^{2+} detection using the MgFe-LDH-modified graphene electrode *via* the potential-resolved mechanism. Reprinted with permission from ref. 64. Copyright 2018, Elsevier. (b) Multiple heavy metal ion detection with an *N*,*N*-dimethyl-*N*-2-propenyl-2-propen-1-aminium chloride homopolymer ionic liquid-doped MgAl-LDH-modified glassy carbon electrode *via* anodic stripping voltammetry. Reprinted with permission from ref. 65. Copyright 2019, Springer.

Besides graphene, ionic liquids with high conductivity have also been applied for developing effective LDH-based electrochemical sensors. Using an *N*,*N*-dimethyl-*N*-2-propenyl-2-propen-1-aminium chloride homopolymer ionic liquid doped MgAl-LDH modified glassy carbon electrode, Zhou *et al.* proposed a high-throughput electrochemical sensor for simultaneous detection of Cd^{2+}, Cu^{2+}, Hg^{2+} and Pb^{2+} based on anodic stripping voltammetry.[65] The peak potentials of Cd^{2+}, Cu^{2+}, Hg^{2+} and Pb^{2+} were −768, +42, +302 and −541 mV with an Ag/AgCl reference electrode (Fig. 4b). The introduction of an ionic liquid not only provides a mesoporous architecture, but also facilitates the electron transfer. As a result, sensitive detection of Cd^{2+}, Cu^{2+}, Hg^{2+} and Pb^{2+} was realized with LODs of 250, 25, 250 and 16 ng L^{-1}, respectively. The proposed approach has been applied for heavy metal analysis in spiked black tea extracts and dried tangerine peel.

3.4 Atomic absorption spectrometry

As the National Standard protocol (GB/T 17141-1997), atomic absorption spectrometry shows high sensitivity and accuracy toward heavy metal ions. Similar to X-ray fluorescence, atomic absorption spectrometry utilizes intraatomic electron transition, which provides characteristic spectral lines for certain heavy metals. And such an electron transition is not affected by the valence state. Despite the requirement of a special ionic source, the high sensitivity and intrinsic multiple target sensing character make atomic absorption spectrometry suitable for the detection of heavy metal ions with low concentrations.

To achieve sensitive detection with LDHs, a simple route is to enrich heavy metal ions by surface modification. In this case, organic molecules and inorganic nanoparticles have been investigated. In addition, in order to simplify the separation, Fe_3O_4 magnetic nanoparticles were accompanied to produce LDH adsorbents. For example, through the coprecipitation method, Fe_3O_4 nanoparticle decorated NiAl-LDHs were prepared for Cd^{2+} and Pb^{2+} analysis with the assistance of micro solid phase extraction by Arghavani-Beydokhti *et al.*[66] The large specific surface area of the as-prepared Fe_3O_4–NiAl-LDH hybrid materials allowed for

effective capture of Cd^{2+} and Pb^{2+}. After extraction and magnetic separation, the heavy metal contents were determined with flame atomic absorption spectrometry by acidic dissolution. Under the optimal conditions, sensitive Cd^{2+} and Pb^{2+} analysis with good linearity in the concentration range of 0.75–35 ng mL^{-1} and 4.0–370 ng mL^{-1} was realized. The LODs toward Cd^{2+} and Pb^{2+} were found to be 0.25 and 1.0 ng mL^{-1}, respectively.

Despite the magnetic separation character, the enrichment capability of Fe_3O_4-LDH hybrid materials is still poor. To further enhance the capture and detection of heavy metal ions, organo-functionalization of LDHs was applied. With the co-functionalization of a surfactant and polymer, Rajabi *et al.* developed two kinds of Fe_3O_4-LDH nanosorbents for the detection of heavy metal ions.[67,68] Note that the chelation between organic molecules and heavy metal ions promotes their pre-concentration and detection; polymers with strong coordinating atoms (*e.g.*, N and S) were thus chosen. To prevent the isolation of the polymer or surfactant, the surfactant-embedded polymer was generally prepared first. Using sodium dodecyl benzene sulfonate (DBSNa) embedded polyaniline (PA) as the co-sorbent, they proposed a PA–DBSNa–Fe_3O_4–ZnAl-LDH nanosorbent for the pre-concentration and detection of Ni^{2+}, Pb^{2+}, Co^{2+}, and Cd^{2+}.[67] Such a high throughput analysis capability is partially due to the wide chelation between N and metal ions. After optimization, linear detection of Ni^{2+}, Pb^{2+}, Co^{2+} and Cd^{2+} was achieved in the concentration range of 5–500, 7–750, 5–500 and 3–100 ng mL^{-1}, respectively. With the integration of a CO_2-effervescence assisted dispersive micro solid-phase extraction procedure, sensitive detection of Ni^{2+}, Pb^{2+}, Co^{2+} and Cd^{2+} was realized with LODs of 1.4, 2.1, 1.5 and 0.9 ng mL^{-1}, respectively. When changing PA into polythiophene (PTH, S as the coordinating atom), a selective PTH–DBSNa–Fe_3O_4–ZnAl-LDH nanosorbent for Ni^{2+} and Cd^{2+} was proposed.[68] With the assistance of ultrasound-assisted dispersive micro solid phase extraction and flame atomic absorption spectrometry, they achieved sensitive Ni^{2+} and Cd^{2+} detection in the concentration ranges of 5–300 and 2.5–100 ng mL^{-1} with good linearity. The LODs towards Ni^{2+} and Cd^{2+} were 1.3 and 0.7 ng mL^{-1}, respectively.

4 Removal of heavy metal ions

The existence of toxic heavy metal ions in polluted environments hinders the utilization of resources, including rivers, farmlands and woods. Therefore, their removal is essential to environmental treatment and recycling of resources. To meet this demand, it is urgent to explore rapid and efficient sorbents for their adsorption, and considerable effort has been devoted to the development of hybrid LDH-based nanosorbents because of the high capture capacity. However, the adsorption mechanisms of heavy metal ions using different LDH-based nanosorbents are not exactly the same. In this section, we will introduce LDH-based removal of heavy metal ions in two categories: reversible adsorption and irreversible mineralization.

4.1 Reversible adsorption

The positive charge and partially empty d orbital make heavy metal ions attracted toward negatively charged and electron-donative species. In consideration of the positively charged LDH layer, intercalated and surface anions are beneficial to interact with heavy metal ions through electrostatic attraction and chelation. Such interactions generally allow for the reversible adsorption of heavy metal ions. In this part, removal of heavy metal ions by reversible adsorption is described based on electrostatic attraction or chelation.

By intercalating carboxyl compounds, LDH-based nanosorbents with improved adsorption capacity toward heavy metal ions are prepared. Small molecules including EDTA and mercaptocarboxylic acid (MPA) have been reported for preparing intercalated LDH nanosorbents toward heavy metal ion removal.[69,70] The introduction of carboxyl groups not only increases the negative charge of LDHs, but also provides more binding sites to heavy metal ions by chelation. As shown in Fig. 5a, using EDTA as the intercalating anion, Liu *et al.* explored MgAl-LDH nanosorbents for the removal of Ni^{2+} with an adsorption capacity of 108.2 mg g^{-1}, which is much higher than that of the bare MgAl-LDHs (23.47 mg g^{-1}).[69] Interestingly, the introduction of the sulfur-containing MPA intercalation anion endowed the nanosorbents with high adsorption capacity for multiple heavy metal ions, including Hg^{2+}, Pb^{2+}, and Cu^{2+}.[70] Under pH 5 working condition, the maximum adsorption capacities for Hg^{2+}, Pb^{2+}, and Cu^{2+} were determined to be 250.30, 122.10, and 105.33 mg g^{-1}, respectively.

In addition to small molecules, carboxylic polymers are also adaptable for LDH modification. For instance, Chen

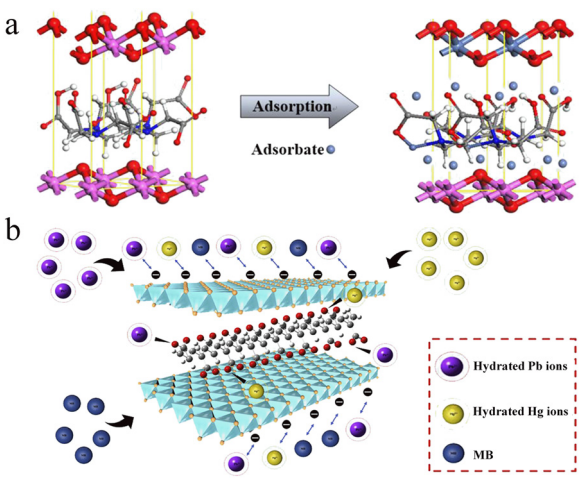

Fig. 5 (a) Schematic diagram of Ni^{2+} adsorption with EDTA-intercalated MgAl-LDH nanosorbents. Reprinted with permission from ref. 69. Copyright 2019, American Chemical Society. (b) Schematic illustration of PAAS EDTA-intercalated MgAl-LDH nanosorbents for the adsorption of Pb^{2+} and Hg^{2+}. Reprinted with permission from ref. 71. Copyright 2021, Elsevier.

et al. reported sodium polyacrylate (PAAS) intercalated MgAl-LDHs for the effective removal of Pb^{2+} and Hg^{2+} from waste water (Fig. 5b).[71] The PAAS intercalation changes the surface charge and hydrophilicity of LDHs, which benefits the adsorption of Pb^{2+} and Hg^{2+}. The maximum adsorption capacities were determined to be 345.4 and 142.7 mg g^{-1}, respectively. Peptides with carboxyl residues can also act as effective intercalation anions. Using polyaspartic acid intercalated MgAl-LDHs, Yin *et al.* constructed eco-friendly nanosorbents for the removal of heavy metal ions from aqueous solutions.[72] The orderly carboxylic groups in polyaspartic acid facilitate the inner-sphere complexation, which promotes the treatment of heavy metal ions. The maximum adsorption capacities toward Pb^{2+} and Hg^{2+} were 229.2 and 208.6 mg g^{-1}, respectively.

Beyond carboxyl compounds, highly charged inorganic anions have also been utilized for intercalating LDHs.[73] Zhou *et al.* found that the intercalation of sulfide anions (S^{2-}) enhanced the adsorption of Co^{2+} and Ni^{2+} with increased electrostatic attraction.[74] The maximum adsorption capacities toward Co^{2+} and Ni^{2+} were 88.6 and 76.2 mg g^{-1}, respectively. Interestingly, this nanosorbent allowed for the adsorption of an anionic heavy metal (CrO_4^{2-}). The unusual adsorption of CrO_4^{2-} was attributed to the anionic exchange between S^{2-} and CrO_4^{2-}. By using MoS_4^{2-} as the intercalation anion, Rathee *et al.* proposed a NiFeTi-LDH nanosorbent for effective removal of heave metal ions within 10 min.[75] In their work, the responses toward various metal ions were listed as the following order: $Ni^{2+} < Cu^{2+} < Zn^{2+} < Fe^{3+} < Pb^{2+} < Ag^{+}$. The maximum adsorption capacities toward Pb^{2+} and Ag^{+} were 856 and 653 mg g^{-1}, respectively.

The nanomaterial-LDH hybrids have also been applied for the exploration of efficient nanosorbents.[38,76,77] By grafting thiol- or amino-functionalized grapheme oxide onto MgAl-LDHs, Liao *et al.* reported two kinds of nanosorbents for the adsorption of Cu^{2+} and Cd^{2+}.[76] The adsorption isotherms could be well fitted by both Langmuir and Freundlich models. The maximum adsorption capability toward Cu^{2+} didn't show distinct variations by thiol (234.80 mg g^{-1}) or amino (204.80 mg g^{-1}) functionalization. In contrast, the maximum adsorption capability toward Cd^{2+} with thiol functionalization (102.77 mg g^{-1}) was about triple that of amino (37.99 mg g^{-1}) functionalization. The enhanced Cd^{2+} capture might be attributed to the synergistic effect of LDH and thiolated grapheme oxide. With the use of lignin derived carbon and CaFeAl-LDHs, Chen *et al.* explored a nanosorbent for the removal of high valence metals (U(VI) and Cr(VI)).[38] They found that the plasma-regulated defect in carbon was critical to the adsorption performance due to the changed complexation between metal ions and carbon. Under the optimal condition, nanosorbents were acquired with a maximum adsorption capability of 267.65 mg g^{-1} toward U(VI). Similarly, with the use of glycerol-modified CaAl-LDHs, Zou *et al.* proposed a U(VI) nanosorbent with a maximum adsorption capability of 266.5 mg g^{-1}.[78] Changing CaAl-LDHs into NiAl-LDHs, the maximum adsorption capability decreased to 142.3 mg g^{-1} because the Ca–O group shows high-activity toward U(VI).

4.2 Irreversible mineralization

As mentioned above, heavy metal ions have a devastating effect on ecological systems because of their nonbiodegradability, bioaccumulation, and high toxicity. For example, Cd^{2+} contaminated agriculture soil causes severe health risk to humans through the food chain, and it becomes a global issue because of the anthropogenic and geographic activity. Despite the development of various LDH-based nanosorbents, many of them only capture heavy metal ions by reversible adsorption, which is difficult to deal with heavy metal ions in complicated environments, such as soil. Therefore, the effective removal or stabilization of heavy metal ions is critical to reduce the ecological risk.

A general strategy for permanent fixation is changing heavy metal ions into a part of materials by chemical reaction, which avoids the involvement of reversible attraction or chelation.[28,79] To meet this demand, considerable effort has been dedicated to the exploration of chemical reduction and ion exchange based approaches. For instance, using $Mo_3S_{13}^{2-}$ anion intercalated MgAl-LDHs (Mo_3S_{13}-LDH), Yang *et al.* developed effective nanosorbents for permanent Ag^{+} fixation with a maximum adsorption capability of 1073 mg g^{-1}.[80] The as-prepared Mo_3S_{13}-LDH captured Ag^{+} through two mechanisms: 1. formation of Ag_2S due to Ag–S complexation and precipitation; 2. reduction of Ag^{+} to metallic silver (Ag^0), as shown in Fig. 6a. The Mo_3S_{13}-LDH also showed excellent capture capability for Hg^{2+} (594 mg g^{-1}), with high selectivity response toward heavy metal ions in the following order: Ag^{+} (K_d 5.4×10^7 mL g^{-1}) > Hg^{2+} (3.6×10^5 mL g^{-1}) > Cu^{2+} (7.0×10^4 mL g^{-1}) > Pb^{2+} (1.4×10^3 mL g^{-1}) ≥ Co^{2+} (71 mL g^{-1}), Ni^{2+} (81 mL g^{-1}), Zn^{2+} (86 mL g^{-1}), Cd^{2+} (84 mL g^{-1}). It was noticed that the Ag^{+} removal rates remained >99.9% even with 500-fold Cu^{2+} existence, suggesting the practical potential of selective Ag^{+} extraction in Cu-rich environments.

Another effective strategy is to fix heavy metal ions by ion exchange-based replacement. The cationic exchange processes have been widely applied in divalent heavy metal ion detection using ZnS or MnZnS quantum dots.[49] For LDH-based mineralization cases, the divalent metal in the layer is replaced by the toxic heavy metal ions, which results in the formation of a new LDH layer (Fig. 6b).[87] In contrast, the trivalent metal in the layer of LDHs is difficult to replace because of the high coordination number and large steric hindrance. Such a replacement reaction is generally related to several parameters, including ionic size and coordination number of metal ions, K_{sp} values of metal hydroxides and corresponding LDHs, and defect of LDHs. In general, the replacement is only triggered by heavy metal ions with similar ionic sizes and coordination number. In addition, the replacement is promoted with the increased K_{sp} difference between metal hydroxides and corresponding LDHs. In

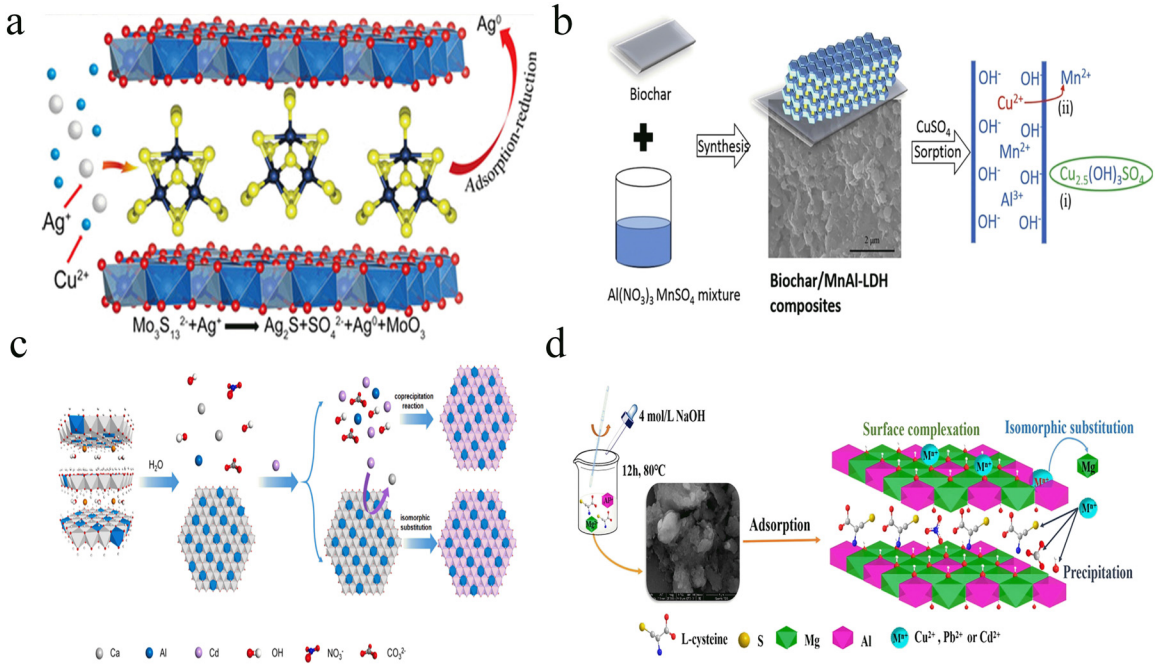

Fig. 6 (a) Schematic of Mo_3S_{13}-LDH-assisted conversion of Ag^+/Ag^0. Reprinted with permission from ref. 80. Copyright 2022, Wiley-VCH. (b) Schematic diagram of ion exchange-mediated Cu removal with MnAl-LDHs. Reprinted with permission from ref. 87. Copyright 2021, Elsevier. (c) Schematic diagram of the proposed mechanism for the formation of CdAl-LDH. Reprinted with permission from ref. 25. Copyright 2021, Elsevier. (d) Schematic illustration of the adsorption of Cu^{2+}, Pb^{2+} and Cd^{2+} using L-cysteine-intercalated MgAl-LDHs. Reprinted with permission from ref. 85. Copyright 2020, Elsevier.

addition, replacement reaction rate is partially enhanced by the increased defect of LDHs. On the basis of this fixation mechanism, intercalation with anions, small molecules or polymers is not necessary.

For example, Kong *et al.* reported a rapid and efficient *in situ* Cd^{2+} mineralization approach using CaAl-LDHs as the stabilizer.[25] As shown in Fig. 6c, the immobilization of Cd^{2+} was realized by two steps: a. fast trapping of Cd^{2+} onto the CaAl-LDH surface by adsorption; b. *in situ* ion exchange-induced reconstruction of CdAl-LDHs. The adsorption of Cd^{2+} finished within 5 min, which is demonstrated by inductively coupled plasma optical-emission spectrometry (ICP-OES). According to the transmission electron microscope (TEM) and X-ray diffraction (XRD) results, the intermediate underwent metal exchange and complete formation of CdAl-LDHs with a 30 min reaction window. With the integration of the cation exchange mechanism, the CaAl-LDHs showed super-stable mineralization of Cd^{2+} in solution with a 592 mg g^{-1} adsorption capacity. Using CaAl-LDHs as the stabilizer, 96.9% Cd^{2+} immobilization efficiency in soil remediation was achieved. Importantly, the scaling-up production of CaAl-LDHs reached 3000 tons per year, indicating the potential application of efficient remediation of Cd contaminated soil with CaAl-LDHs. By employing CaFe-LDHs as the stabilizer, Chi *et al.* realized efficient mineralization of Ni^{2+} with a similar mechanism.[88] They also found that the MgFe-LDHs displayed lower removal capacity (184 mg g^{-1}) than CaFe-LDHs (321 mg g^{-1}). As is known, Ca^{2+} possesses a larger radius compared with Mg^{2+} and CaFe-LDHs show a higher K_{sp} value than MgFe-LDHs. Consequently, the CaFe-LDHs easily convert into NiAl-LDHs in comparison to MgFe-LDHs.

Except Ca^{2+} and Ni^{2+}, other divalent heavy metal ions (*e.g.*, Cu^{2+} and Pb^{2+}) can also be trapped and immobilized by Ca-containing or Mg-containing LDHs.[79,81,83] As indicated in Zhang's work, the CaAl-LDHs also showed a high maximum adsorption capability of 381.9 mg g^{-1} toward Cu^{2+} through the Langmuir model.[82] However, it was still much lower than that of Cd^{2+} (1035.4 mg g^{-1}). In spite of the similar adsorption kinetics, the different surface compositions may lead to diverse cation exchange efficiencies. For Cd^{2+} assays, no $CdCO_3$ or $Cd(OH)_2$ was observed with XRD. In contrast, the $Cu(OH)_2$ signal was easily observed after adsorption in Cu^{2+} assays. The formed $Cu(OH)_2$ may hinder the rapid cation exchange and subsequent formation of CuAl-LDHs. Therefore, CaAl-LDHs showed high adsorption capability toward Cd^{2+}. With the intercalation of thiolates, an enhanced adsorption capacity was observed due to the assistance of precipitation of metal sulfide and surface complexation (Fig. 6d).[85] To facilitate the comparison of different LDH nanosorbents, the adsorption performances are summarized in Table 1. The adsorption capacity (q_e) could be calculated with the following equation: $q_e = [(c_0 - c_e)V]/m$, where c_0 (mg L^{-1}) and c_e (mg L^{-1}) are the concentrations of heavy metal ions before and after adsorption, V (mL) is the volume of heavy metal ion solution, and m (g) is the dosage of LDH nanosorbents.

Table 1 Summary of the adsorption performances of LDH-based nanosorbents

#	Adsorbent	Heavy metal ions	Equilibrium time (min)	Adsorption capacity (mg g^{-1})	C_0, C_e (mg L^{-1})	Ref.
1	FeMg LDH@bentonite	Cd^{2+}, Pb^{2+}	Cd^{2+} 960 Pb^{2+} 480	Cd^{2+} 510.2 Pb^{2+} 1397.62	Cd^{2+} 150, 21.5 Pb^{2+} 300, 9.97	81
2	MPA–MgAl LDH	Hg^{2+}, Pb^{2+}, Cu^{2+}	Hg^{2+} 30 Pb^{2+} 50 Cu^{2+} 50	Hg^{2+} 250.30 Pb^{2+} 122.10 Cu^{2+} 105.33	Hg^{2+} 50, 8.934 Pb^{2+} 50, 25.58 Cu^{2+} 50, 28.93	70
3	CaAl LDH	Cd^{2+}, Cu^{2+}	Cd^{2+} 180 Cu^{2+} 10	Cd^{2+} 1035.4 Cu^{2+} 381.9	Cd^{2+} 500, 17.7 Cu^{2+} 200, 9.05	82
4	FeMnMg LDH	Pb^{2+}	Pb^{2+} 120	Pb^{2+} 421.42	Pb^{2+} 500, 78.58	83
5	MgAl LDH@RHB	Cd^{2+}, Cu^{2+}	Cd^{2+} 300 Cu^{2+} 300	Cd^{2+} 125.34 Cu^{2+} 104.34	Cd^{2+} 200, 60.8 Cu^{2+} 200, 113.3	84
6	Fe_3O_4–$FeMoS_4$–MgAl LDH	Pb^{2+}, Cd^{2+}, Cu^{2+}	Pb^{2+} 60 Cd^{2+} 60 Cu^{2+} 60	Pb^{2+} 190.75 Cd^{2+} 140.50 Cu^{2+} 110.25	Pb^{2+} 300, 14 Cd^{2+} 300, 89.3 Cu^{2+} 300, 134	77
7	MgAl-Cys-LDH	Pb^{2+}, Cd^{2+}, Cu^{2+}	Pb^{2+} 180 Cd^{2+} 100 Cu^{2+} 90	Pb^{2+} 186.2 Cd^{2+} 93.11 Cu^{2+} 58.07	Pb^{2+} 500, 34.5 Cd^{2+} 300, 67.2 Cu^{2+} 300, 154	85
8	PASP-MgAl LDH	Pb^{2+}, Hg^{2+}	Pb^{2+} 40 Hg^{2+} 40	Pb^{2+} 229.2 Hg^{2+} 208.6	Pb^{2+} 10, 0.003 Hg^{2+} 10, 0.007	72
9	LDH@GO–SH LDH@GO–NH_2	Cd^{2+} Cu^{2+}	Cd^{2+} 60 Cu^{2+} 60	Cd^{2+} 102.77 Cu^{2+} 204.08	Cd^{2+} 100, 48.6 Cu^{2+} 200, 97.6	76
10	CNF-NiAl LDH	Cu^{2+}, Cr(VI)	Cu^{2+} 120 Cr(VI) 120	Cu^{2+} 219.6 Cr(VI) 341.2	Cu^{2+} 74, 30 Cr(VI) 98, 30	86
11	MoS_4^{2-}–NiFeTi LDH–NO_3	Pb^{2+}, Ag^{+}	Pb^{2+} 80 Ag^{+} 80	Pb^{2+} 653 Ag^{+} 856	Pb^{2+} 100, 0.43 Ag^{+} 100, 0.001	75
12	PAAS-MgAl LDH	Pb^{2+}, Hg^{2+}	Pb^{2+} 100 Hg^{2+} 90	Pb^{2+} 345.4 Hg^{2+} 142.7	Pb^{2+} 50, 15.46 Hg^{2+} 50, 20.56	71
13	LDH@LDC	U(VI), Cr(VI)	U(VI) 200 Cr(VI) 100	U(VI) 443.41 Cr(VI) 274.48	U(VI) 30, 2.55 Cr(VI) 30, 14.34	38
14	Fe_3O_4–MgAl LDH	Pb^{2+}, Cd^{2+}, Cu^{2+}	Cu^{2+} 240 Cd^{2+} 240 Pb^{2+} 180	Pb^{2+} 266.6 Cd^{2+} 74.06 Cu^{2+} 64.66	Pb^{2+} 180, 105 Cd^{2+} 180, 135 Cu^{2+} 180, 152	79
15	$Mo_3S_{13}^{2-}$–MgAl LDH	Hg^{2+}, Ag^{+}	Hg^{2+} 100 Ag^{+} 100	Hg^{2+} 594 Ag^{+} 1073	Hg^{2+} 10.8, 0.03 Ag^{+} 10.9, 0.001	80

The mineralization reaction not only achieves the fixation of heavy metal ions, but also produces new LDHs, sometimes with unexpected chemical reactivity. It is reported that transition metal-based LDHs present efficient photocatalytic activities due to the strong metal-to-metal charge-transfer.[89,90] Interestingly, the heavy metal pollutants (*e.g.*, Ni, Pb, Co and Cu) contribute high metal-to-metal charge-transfer efficiency in LDHs. After mineralization, the formed ternary LDHs might be good catalysts for realizing photocatalytic application. In Chi's work, the formed ternary NiCaFe-LDH intermediates showed high photocatalytic activity toward CO_2 reduction.[88] Under light irradiation, CO_2 was converted into CO and CH_4. Similarly, after the adsorption of Hg^{2+}, Pb^{2+}, and Cu^{2+} onto MPA-LDHs, photocatalytic degradation of organic dyes with high efficiency (>95%) was achieved based on the formed LDH intermediates.[70] Therefore, the LDH-based nanosorbents not only remove heavy metal pollutants, but also provide feasibility to yield effective photocatalysts.

5 Conclusion and perspectives

In this review, we have provided an overview on the recent advances in the detection and removal of heavy metal ions based on LDHs. Based on the enrichment effect, most LDH-based nanosensors show enhanced sensitivity toward toxic heavy metal ions by integrating proper detection techniques. The anion intercalation endows LDH-based nanosorbents good adsorption capabilities through electrostatic attraction and chelation. With further cation exchange amplification, some LDH-based stabilizers allow the permanent immobilization of heavy metal ions in aqueous media and soil remediation.

Despite the successful exploration of effective LDH-based nanosensors and nanosorbents for the detection and removal of heavy metal ions, some challenges regarding this research area still exist. For LDH-based assays, several limitations still exist and need to be addressed in future. Here, we'd like to share our viewpoints of challenges focusing on sensing and mineralization performances of LDHs.

1) Selective pre-concentration of specific heavy metal ions. Although numbers of LDH-based nanosensors with high enrichment capabilities have been reported, most of them can't selectively capture one metal ion. For example, intercalated LDHs usually adsorb two or more heavy metal ions with comparable adsorption capability. In this case, the co-concentrated metal ion may affect the detection of target ions. On the other hand, the occupied binding site may have the side effect of weakening the sensitivity. The modified LDHs capture metal ions through electrostatic attraction and

chelation, and these two pathways have non-unified contribution. The exploration of LDH nanosensors with designed pre-concentration capability toward expected heavy metal ions might be an interesting research direction in future.

2) Unclear mechanism of mineralization diversity. It is reported that Ca-containing or Mg-containing LDHs show non-uniform removal efficiencies toward different heavy metal ions. And in general, the capture capability toward Cd^{2+} is much higher than that for other divalent metal ions with the same LDHs. Meanwhile, different LDHs also display different capture capabilities toward the same metal ions. That is, the cation exchange behaviour is dependent on the atomic structure of metal ions. However, the relationship between cation exchange efficiency and atomic structure is missing, which limits the development of universal LDH-based nanosorbents and stabilizers for immobilizing heavy metal ions.

3) Direct visualization of the mineralization process. As referred in the last section, the permanent immobilization of heavy metal ions is promoted by cation exchange reaction, and the time-dependent ICP-OES, XRD and TEM results have been provided. These results, however, cannot represent the adsorption and *in situ* exchange process. And the sample preparation process may change the structure of LDHs, which brings in false results. Therefore, direction visualization of adsorption and cation exchange processes is essential to illustrate the mineralization mechanism. In addition, the kinetics behaviour might benefit the deep understanding of mineralization diversity toward different heavy metal ions.

Conflicts of interest

The authors declare no conflict of interest.

Acknowledgements

This work was supported by the National Natural Science Foundation of China (22074005 and 21974008) and the Natural Science Foundation of Beijing Municipality (2202038).

References

1 Y. Shen, C. Nie, Y. Wei, Z. Zheng, Z.-L. Xu and P. Xiang, FRET-based innovative assays for precise detection of the residual heavy metals in food and agriculture-related matrices, *Coord. Chem. Rev.*, 2022, **469**, 214676.
2 O. Buhari, A. Atanda, T. Alzharani and R. Faillace, Exposure to heavy metals may increase cardiovascular risk by elevation of serum lipid levels and hemoglobin a1c: a national health and nutrition examination survey based study, *J. Am. Coll. Cardiol.*, 2019, **73**, 1882.
3 J. H. Chen, K. Pelka and N. Hacohen, Heavy Metal Enlightens Tumor Immunity, *Cell*, 2017, **169**, 567–569.
4 K. D. Whitaker, E. A. Ross, J. E. Klaunig, T. Singh, R. Veggeberg, K. Alpaugh and L. J. Goldstein, Assessing association of heavy metal levels in urine and sera with neurotoxicity in breast cancer(BC) patients undergoing adjuvant/neoadjuvant chemotherapy, *J. Clin. Oncol.*, 2022, **40**, e12510.
5 Y. Zhao, J. Gao, Z. Wang, H. Dai and Y. Wang, Responses of bacterial communities and resistance genes on microplastics to antibiotics and heavy metals in sewage environment, *J. Hazard. Mater.*, 2021, **402**, 123550.
6 K. Yin, Q. Wang, M. Lv and L. Chen, Microorganism remediation strategies towards heavy metals, *Chem. Eng. J.*, 2019, **360**, 1553–1563.
7 M. Yin, X. Bai, D. Wu, F. Li, K. Jiang, N. Ma, Z. Chen, X. Zhang and L. Fang, Sulfur-functional group tunning on biochar through sodium thiosulfate modified molten salt process for efficient heavy metal adsorption, *Chem. Eng. J.*, 2022, **433**, 134441.
8 K. Gupta, P. Joshi, R. Gusain and O. P. Khatri, Recent advances in adsorptive removal of heavy metal and metalloid ions by metal oxide-based nanomaterials, *Coord. Chem. Rev.*, 2021, **445**, 214100.
9 R. Wang, R. Liang, T. Dai, J. Chen, X. Shuai and C. Liu, Pectin-based adsorbents for heavy metal ions: A review, *Trends Food Sci. Technol.*, 2019, **91**, 319–329.
10 C. Kang, S. Tao, F. Yang and B. Yang, Aggregation and luminescence in carbonized polymer dots, *Aggregate*, 2022, **3**, e169.
11 H. Zhu, J. Fan, B. Wang and X. Peng, Fluorescent, MRI, and colorimetric chemical sensors for the first-row d-block metal ions, *Chem. Soc. Rev.*, 2015, **44**, 4337–4366.
12 Z. Yuan, N. Cai, Y. Du, Y. He and E. S. Yeung, Sensitive and Selective Detection of Copper Ions with Highly Stable Polyethyleneimine-Protected Silver Nanoclusters, *Anal. Chem.*, 2014, **86**, 419–426.
13 W. Li, Y.-Y. Liu, Y. Bai, J. Wang and H. Pang, Anchoring ZIF-67 particles on amidoximerized polyacrylonitrile fibers for radionuclide sequestration in wastewater and seawater, *J. Hazard. Mater.*, 2020, **395**, 122692.
14 X. Chen, W. Li, G. Zhang, F. Sun, Q. Jing and H. Pang, Highly stable and activated Cerium-based MOFs superstructures for ultrahigh selective uranium (VI) capture from simulated seawater, *Mater. Today Chem.*, 2022, **23**, 100705.
15 F. Yang, M. Du, K. Yin, Z. Qiu, J. Zhao, C. Liu, G. Zhang, Y. Gao and H. Pang, Applications of Metal-Organic Frameworks in Water Treatment: A Review, *Small*, 2022, **18**, 2105715.
16 B. Wang, Q. Yang, C. Guo, Y. Sun, L.-H. Xie and J.-R. Li, Stable Zr(IV)-Based Metal–Organic Frameworks with Predesigned Functionalized Ligands for Highly Selective Detection of Fe(III) Ions in Water, *ACS Appl. Mater. Interfaces*, 2017, **9**, 10286–10295.
17 R. Gao, D. Yan and X. Duan, Layered double hydroxides-based smart luminescent materials and the tuning of their excited states, *Cell Rep. Phys. Sci.*, 2021, **2**, 100536.
18 F. Mao, P. Hao, Y. Zhu, X. Kong and X. Duan, Layered double hydroxides: Scale production and application in soil

remediation as super-stable mineralizer, *Chin. J. Chem. Eng.*, 2022, **41**, 42–48.

19 Z. Gao, B. Du, G. Zhang, Y. Gao, Z. Li, H. Zhang and X. Duan, Adsorption of pentachlorophenol from Aqueous Solution on Dodecylbenzenesulfonate Modified Nickel –Titanium Layered Double Hydroxide Nanocomposites, *Ind. Eng. Chem. Res.*, 2011, **50**, 5334–5345.

20 L. Lv, J. He, M. Wei and X. Duan, Kinetic Studies on Fluoride Removal by Calcined Layered Double Hydroxides, *Ind. Eng. Chem. Res.*, 2006, **45**, 8623–8628.

21 D. Zhou, P. Li, X. Lin, A. McKinley, Y. Kuang, W. Liu, W.-F. Lin, X. Sun and X. Duan, Layered double hydroxide-based electrocatalysts for the oxygen evolution reaction: identification and tailoring of active sites, and superaerophobic nanoarray electrode assembly, *Chem. Soc. Rev.*, 2021, **50**, 8790–8817.

22 X. He, X. Qiu, C. Hu and Y. Liu, Treatment of heavy metal ions in wastewater using layered double hydroxides: A review, *J. Dispersion Sci. Technol.*, 2018, **39**, 792–801.

23 X. Feng, R. Long, L. Wang, C. Liu, Z. Bai and X. Liu, A review on heavy metal ions adsorption from water by layered double hydroxide and its composites, *Sep. Purif. Technol.*, 2022, **284**, 120099.

24 S.-S. Li, M. Jiang, T.-J. Jiang, J.-H. Liu, Z. Guo and X.-J. Huang, Competitive adsorption behavior toward metal ions on nano-Fe/Mg/Ni ternary layered double hydroxide proved by XPS: Evidence of selective and sensitive detection of Pb(II), *J. Hazard. Mater.*, 2017, **338**, 1–10.

25 X. Kong, R. Ge, T. Liu, S. Xu, P. Hao, X. Zhao, Z. Li, X. Lei and H. Duan, Super-stable mineralization of cadmium by calcium-aluminum layered double hydroxide and its large-scale application in agriculture soil remediation, *Chem. Eng. J.*, 2021, **407**, 127178.

26 Y. Dong, X. Kong, X. Luo and H. Wang, Adsorptive removal of heavy metal anions from water by layered double hydroxide: A review, *Chemosphere*, 2022, **303**, 134685.

27 Z. Tang, Z. Qiu, S. Lu and X. Shi, Functionalized layered double hydroxide applied to heavy metal ions absorption: A review, *Nanotechnol. Rev.*, 2020, **9**, 800–819.

28 X. Guan, X. Yuan, Y. Zhao, H. Wang, H. Wang, J. Bai and Y. Li, Application of functionalized layered double hydroxides for heavy metal removal: A review, *Sci. Total Environ.*, 2022, **838**, 155693.

29 H. Sohrabi, A. Khataee, S. Ghasemzadeh, M. R. Majidi and Y. Orooji, Layer double hydroxides (LDHs)- based electrochemical and optical sensing assessments for quantification and identification of heavy metals in water and environment samples: A review of status and prospects, *Trends Environ. Anal. Chem.*, 2021, **31**, e00139.

30 M. Laipan, J. Yu, R. Zhu, J. Zhu, A. T. Smith, H. He, D. O'Hare and L. Sun, Functionalized layered double hydroxides for innovative applications, *Mater. Horiz.*, 2020, **7**, 715–745.

31 J. Yu, Q. Wang, D. O'Hare and L. Sun, Preparation of two dimensional layered double hydroxide nanosheets and their applications, *Chem. Soc. Rev.*, 2017, **46**, 5950–5974.

32 F. Pan, Y. Zhang, Z. Yuan and C. Lu, Sensitive and Selective Carmine Acid Detection Based on Chemiluminescence Quenching of Layer Doubled Hydroxide–Luminol–H_2O_2 System, *ACS Omega*, 2018, **3**, 18836–18842.

33 F. Pan, Y. Zhang, Z. Yuan and C. Lu, Determination of alizarin red S based on layered double hydroxides-improved chemiluminescence from hydrogen peroxide and luminol, *Anal. Methods*, 2017, **9**, 6468–6473.

34 Z.-z. Yang, J.-j. Wei, G.-m. Zeng, H.-q. Zhang, X.-f. Tan, C. Ma, X.-c. Li, Z.-h. Li and C. Zhang, A review on strategies to LDH-based materials to improve adsorption capacity and photoreduction efficiency for CO_2, *Coord. Chem. Rev.*, 2019, **386**, 154–182.

35 C. Taviot-Guého, V. Prévot, C. Forano, G. Renaudin, C. Mousty and F. Leroux, Tailoring Hybrid Layered Double Hydroxides for the Development of Innovative Applications, *Adv. Funct. Mater.*, 2018, **28**, 1703868.

36 C. Li, M. Wei, D. G. Evans and X. Duan, Layered double hydroxide-based nanomaterials as highly efficient catalysts and adsorbents, *Small*, 2014, **10**, 4469–4486.

37 G. Wang and Z. Jin, Oxygen-vacancy-rich cobalt–aluminium hydrotalcite structures served as high-performance supercapacitor cathode, *J. Mater. Chem. C*, 2021, **9**, 620–632.

38 H. Chen, Z. Gong, Z. Zhuo, X. Zhong, M. Zhou, X. Xiang, Z. Zhang, Y. Liu and Y. Chen, Tunning the defects in lignin-derived-carbon and trimetallic layered double hydroxides composites (LDH@LDC) for efficient removal of U(VI) and Cr(VI) in aquatic environment, *Chem. Eng. J.*, 2022, **428**, 132113.

39 X. Zhang, W. Zhou, Z. Yuan and C. Lu, Colorimetric detection of biological hydrogen sulfide using fluorosurfactant functionalized gold nanorods, *Analyst*, 2015, **140**, 7443–7450.

40 Z. Yuan, F. Lu, M. Peng, C.-W. Wang, Y.-T. Tseng, Y. Du, N. Cai, C.-W. Lien, H.-T. Chang, Y. He and E. S. Yeung, Selective Colorimetric Detection of Hydrogen Sulfide Based on Primary Amine-Active Ester Cross-Linking of Gold Nanoparticles, *Anal. Chem.*, 2015, **87**, 7267–7273.

41 D. Xu, S. Yu, Y. Yin, S. Wang, Q. Lin and Z. Yuan, Sensitive Colorimetric Hg^{2+} Detection via Amalgamation-Mediated Shape Transition of Gold Nanostars, *Front. Chem.*, 2018, **6**, 566.

42 Z.-F. Pu, B.-C. Wu, Y.-H. Tan, Q.-L. Wen, J. Ling and Q.-E. Cao, Selective Aggregation of Silver Nanoprisms Induced by Monohydrogen Phosphate and its Application for Colorimetric Detection of Chromium (III) Ions, *J. Anal. Test.*, 2021, **5**, 225–234.

43 Y. Zhang, Y.-L. Li, S.-H. Cui, C.-Y. Wen, P. Li, J.-F. Yu, S.-M. Tang and J.-B. Zeng, Distance-Based Detection of Ag^{+} with Gold Nanoparticles-Coated Microfluidic Paper, *J. Anal. Test.*, 2021, **5**, 11–18.

44 N. Wang, J. Sun, H. Fan and S. Ai, Anion-intercalated layered double hydroxides modified test strips for detection of heavy metal ions, *Talanta*, 2016, **148**, 301–307.

45 S. Tang, Y. Chang, G. H. Chia and H. K. Lee, Selective extraction and release using (EDTA-Ni)-layered double

hydroxide coupled with catalytic oxidation of 3,3′,5,5′-tetramethylbenzidine for sensitive detection of copper ion, *Anal. Chim. Acta*, 2015, **885**, 106–113.

46 S. Tang, J. Sun, Y. Li, D. Xia, T. Qi, K. Liu, H. Deng, W. Shen and H. K. Lee, pH-dependent selective ion exchange based on (ethylenediamintetraacetic acid-nickel)-layered double hydroxide to catalyze the polymerization of aniline for detection of Cu^{2+} and Fe^{3+}, *Talanta*, 2018, **187**, 287–294.

47 J.-J. Zheng, W.-C. Liu, F.-N. Lu, Y. Tang and Z.-Q. Yuan, Recent Progress in Fluorescent Formaldehyde Detection Using Small Molecule Probes, *J. Anal. Test.*, 2022, **6**, 204–215.

48 Z. Yuan, Y.-C. Chen, H.-W. Li and H.-T. Chang, Fluorescent silver nanoclusters stabilized by DNA scaffolds, *Chem. Commun.*, 2014, **50**, 9800–9815.

49 J. Liu, X. Zhao, H. Xu, Z. Wang and Z. Dai, Amino Acid-Capped Water-Soluble Near-Infrared Region $CuInS_2$/ZnS Quantum Dots for Selective Cadmium Ion Determination and Multicolor Cell Imaging, *Anal. Chem.*, 2019, **91**, 8987–8993.

50 Z. Yuan, M. Peng, Y. He and E. S. Yeung, Functionalized fluorescent gold nanodots: synthesis and application for Pb^{2+} sensing, *Chem. Commun.*, 2011, **47**, 11981–11983.

51 B. Zawisza, R. Sitko and A. Gagor, Determination of ultra-trace gold in cosmetics using aluminum-magnesium layered double hydroxide/graphene oxide nanocomposite, *Talanta*, 2022, **245**, 123460.

52 S. Omwoma, Trace Metal Detection in Aqueous Reservoirs Using Stilbene Intercalated Layered Rare-Earth Hydroxide Tablets, *J. Anal. Methods Chem.*, 2020, **2020**, 9712872.

53 A. A. Wani, A. M. Khan, Y. K. Manea, M. A. S. Salem and M. Shahadat, Selective adsorption and ultrafast fluorescent detection of Cr(VI) in wastewater using neodymium doped polyaniline supported layered double hydroxide nanocomposite, *J. Hazard. Mater.*, 2021, **416**, 125754.

54 W. Shi, X. Ji, S. Zhang, M. Wei, D. G. Evans and X. Duan, Fluorescence Chemosensory Ultrathin Films for Cd^{2+} Based on the Assembly of Benzothiazole and Layered Double Hydroxide, *J. Phys. Chem. C*, 2011, **115**, 20433–20441.

55 W. Shi, Y. Lin, X. Kong, S. Zhang, Y. Jia, M. Wei, D. G. Evans and X. Duan, Fabrication of pyrenetetrasulfonate/layered double hydroxide ultrathin films and their application in fluorescence chemosensors, *J. Mater. Chem.*, 2011, **21**, 6088–6094.

56 J. Liu, G. Lv, W. Gu, Z. Li, A. Tang and L. Mei, A novel luminescence probe based on layered double hydroxides loaded with quantum dots for simultaneous detection of heavy metal ions in water, *J. Mater. Chem. C*, 2017, **5**, 5024–5030.

57 W. Yang, J. Li, Z. Xu, J. Yang, Y. Liu and L. Liu, A Eu-MOF/EDTA-NiAl-CLDH fluorescent micromotor for sensing and removal of Fe^{3+} from water, *J. Mater. Chem. C*, 2019, **7**, 10297–10308.

58 R. Amini, E. Rahimpour and A. Jouyban, An optical sensing platform based on hexacyanoferrate intercalated layered double hydroxide nanozyme for determination of chromium in water, *Anal. Chim. Acta*, 2020, **1117**, 9–17.

59 Z. Lai, F. Lin, Y. Huang, Y. Wang and X. Chen, Automated Determination of Cd^{2+} and Pb^{2+} in Natural Waters with Sequential Injection Analysis Device Using Differential Pulse Anodic Stripping Voltammetry, *J. Anal. Test.*, 2021, **5**, 60–68.

60 N. Ruecha, N. Rodthongkum, D. M. Cate, J. Volckens, O. Chailapakul and C. S. Henry, Sensitive electrochemical sensor using a graphene–polyaniline nanocomposite for simultaneous detection of Zn(II), Cd(II), and Pb(II), *Anal. Chim. Acta*, 2015, **874**, 40–48.

61 Y.-L. Xie, S.-Q. Zhao, H.-L. Ye, J. Yuan, P. Song and S.-Q. Hu, Graphene/CeO_2 hybrid materials for the simultaneous electrochemical detection of cadmium(II), lead(II), copper(II), and mercury(II), *J. Electroanal. Chem.*, 2015, **757**, 235–242.

62 K. Asadpour-Zeynali and R. Amini, A novel voltammetric sensor for mercury(II) based on mercaptocarboxylic acid intercalated layered double hydroxide nanoparticles modified electrode, *Sens. Actuators, B*, 2017, **246**, 961–968.

63 I. M. Isa, S. N. M. Sharif, N. Hashim and S. A. Ghani, Amperometric determination of nanomolar mercury(II) by layered double nanocomposite of zinc/aluminium hydroxide-3(4-methoxyphenyl)propionate modified single-walled carbon nanotube paste electrode, *Ionics*, 2015, **21**, 2949–2958.

64 Y. Ma, Y. Wang, D. Xie, Y. Gu, X. Zhu, H. Zhang, G. Wang, Y. Zhang and H. Zhao, Hierarchical MgFe-layered double hydroxide microsphere/graphene composite for simultaneous electrochemical determination of trace Pb(II) and Cd(II), *Chem. Eng. J.*, 2018, **347**, 953–962.

65 J. Zhou, G. Sun, J. Pan, Y. Pan, S. Wang and H. Zhai, A nanocomposite consisting of ionic liquid-functionalized layered Mg(II)/Al(III) double hydroxides for simultaneous electrochemical determination of cadmium(II), copper(II), mercury(II) and lead(II), *Microchim. Acta*, 2019, **186**, 767.

66 S. Arghavani-Beydokhti, M. Rajabi and A. Asghari, Application of syringe to syringe dispersive micro-solid phase extraction using a magnetic layered double hydroxide for the determination of cadmium(II) and lead(II) ions in food and water samples, *Anal. Methods*, 2018, **10**, 1305–1314.

67 M. Rajabi, Z. Mollakazemi, M. Hemmati and S. Arghavani-Beydokhti, CO_2-effervescence assisted dispersive micro solid-phase extraction based on a magnetic layered double hydroxide modified with polyaniline and a surfactant for efficient pre-concentration of heavy metals in cosmetic samples, *Anal. Methods*, 2020, **12**, 4867–4877.

68 M. Rajabi, M. Abolhosseini, A. Hosseini-Bandegharaei, M. Hemmati and N. Ghassab, Magnetic dispersive micro-solid phase extraction merged with micro-sampling flame atomic absorption spectrometry using (Zn-Al LDH)-(PTh/DBSNa)-Fe_3O_4 nanosorbent for effective trace determination of nickel(II) and cadmium(II) in food samples, *Microchem. J.*, 2020, **159**, 105450.

69 G. Liu, J. Yang, X. Xu and Z. He, Mg–Al Hydrotalcites Intercalated by Ethylenediaminetetraacetic Acid for Ni(II) Removal from Aqueous Solution, *J. Chem. Eng. Data*, 2019, **64**, 5838–5846.

70 R. Bi, D. Yin, B. Lei, F. Chen, R. Zhang and W. Li, Mercaptocarboxylic acid intercalated MgAl layered double hydroxide adsorbents for removal of heavy metal ions and recycling of spent adsorbents for photocatalytic degradation of organic dyes, *Sep. Purif. Technol.*, 2022, **289**, 120741.

71 M. Chen, R. Bi, R. Zhang, F. Yang and F. Chen, Tunable surface charge and hydrophilicity of sodium polyacrylate intercalated layered double hydroxide for efficient removal of dyes and heavy metal ions, *Colloids Surf., A*, 2021, **617**, 126384.

72 R. Bi, D. Yin, S. Zhang, R. Zhang and F. Chen, Efficient removal of Pb(II) and Hg(II) with eco-friendly polyaspartic acid/ layered double hydroxide by host-guest interaction, *Appl. Clay Sci.*, 2022, **225**, 106536.

73 L. Sellaoui, J. Ali, M. Badawi, A. Bonilla-Petriciolet and Z. Chen, Understanding the adsorption mechanism of Ag^{+} and Hg^{2+} on functionalized layered double hydroxide via statistical physics modeling, *Appl. Clay Sci.*, 2020, **198**, 105828.

74 Y. Zhou, Z. Liu, A. Bo, T. Tana, X. Liu, F. Zhao, S. Sarina, M. Jia, C. Yang, Y. Gu, H. Zheng and H. Zhu, Simultaneous removal of cationic and anionic heavy metal contaminants from electroplating effluent by hydrotalcite adsorbent with disulfide (S^{2-}) intercalation, *J. Hazard. Mater.*, 2020, **382**, 121111.

75 G. Rathee, S. Kohli, A. Awasthi, N. Singh and R. Chandra, MoS_4^{2-} intercalated NiFeTi LDH as an efficient and selective adsorbent for elimination of heavy metals, *RSC Adv.*, 2020, **10**, 19371–19381.

76 W. Liao, D. Bao, H.-q. Li and P. Yang, Cu(II) and Cd(II) removal from aqueous solution with LDH@GO-NH_2 and LDH@GO-SH: kinetics and probable mechanism, *Environ. Sci. Pollut. Res.*, 2021, **28**, 65848–65861.

77 E. S. Behbahani, K. Dashtian and M. Ghaedi, Fe_3O_4-$FeMoS_4$: Promise magnetite LDH-based adsorbent for simultaneous removal of Pb(II), Cd(II), and Cu(II) heavy metal ions, *J. Hazard. Mater.*, 2021, **410**, 124560.

78 Y. Zou, Y. Liu, X. Wang, G. Sheng, S. Wang, Y. Ai, Y. Ji, Y. Liu, T. Hayat and X. Wang, Glycerol-Modified Binary Layered Double Hydroxide Nanocomposites for Uranium Immobilization via Extended X-ray Absorption Fine Structure Technique and Density Functional Theory Calculation, *ACS Sustainable Chem. Eng.*, 2017, **5**, 3583–3595.

79 J. Sun, Y. Chen, H. Yu, L. Yan, B. Du and Z. Pei, Removal of Cu^{2+}, Cd^{2+} and Pb^{2+} from aqueous solutions by magnetic alginate microsphere based on Fe_3O_4/MgAl-layered double hydroxide, *J. Colloid Interface Sci.*, 2018, **532**, 474–484.

80 L. Yang, L. Xie, M. Chu, H. Wang, M. Yuan, Z. Yu, C. Wang, H. Yao, S. M. Islam, K. Shi, D. Yan, S. Ma and M. G. Kanatzidis, $Mo_3S_{13}^{2-}$ Intercalated Layered Double Hydroxide: Highly Selective Removal of Heavy Metals and Simultaneous Reduction of Ag^{+} Ions to Metallic Ag^{0} Ribbons, *Angew. Chem., Int. Ed.*, 2022, **61**, e202112511.

81 X. Guan, X. Yuan, Y. Zhao, J. Bai, Y. Li, Y. Cao, Y. Chen and T. Xiong, Adsorption behaviors and mechanisms of Fe/Mg layered double hydroxide loaded on bentonite on Cd(II) and Pb(II) removal, *J. Colloid Interface Sci.*, 2022, **612**, 572–583.

82 S. Zhang, Y. Chen, J. Li, Y. Li, W. Song, X. Li, L. Yan and H. Yu, Highly efficient removal of aqueous Cu(II) and Cd(II) by hydrothermal synthesized CaAl-layered double hydroxide, *Colloids Surf., A*, 2022, **641**, 128584.

83 H. Zhou, Z. Jiang and S. Wei, A new hydrotalcite-like absorbent FeMnMg-LDH and its adsorption capacity for Pb^{2+} ions in water, *Appl. Clay Sci.*, 2018, **153**, 29–37.

84 A. Li, Y. Zhang, W. Ge, Y. Zhang, L. Liu and G. Qiu, Removal of heavy metals from wastewaters with biochar pyrolyzed from MgAl-layered double hydroxide-coated rice husk: Mechanism and application, *Bioresour. Technol.*, 2022, **347**, 126425.

85 X. Zhang, L. Yan, J. Li and H. Yu, Adsorption of heavy metals by l-cysteine intercalated layered double hydroxide: Kinetic, isothermal and mechanistic studies, *J. Colloid Interface Sci.*, 2020, **562**, 149–158.

86 S. Yu, Y. Liu, Y. Ai, X. Wang, R. Zhang, Z. Chen, Z. Chen, G. Zhao and X. Wang, Rational design of carbonaceous nanofiber/Ni-Al layered double hydroxide nanocomposites for high-efficiency removal of heavy metals from aqueous solutions, *Environ. Pollut.*, 2018, **242**, 1–11.

87 T. Wang, C. Li, C. Wang and H. Wang, Biochar/MnAl-LDH composites for Cu (II) removal from aqueous solution, *Colloids Surf., A*, 2018, **538**, 443–450.

88 H. Chi, J. Wang, H. Wang, S. Li, M. Yang, S. Bai, C. Li, X. Sun, Y. Zhao and Y.-F. Song, Super-Stable Mineralization of Ni^{2+} Ions from Wastewater using CaFe Layered Double Hydroxide, *Adv. Funct. Mater.*, 2022, **32**, 2106645.

89 Y. Zhao, X. Jia, G. I. N. Waterhouse, L.-Z. Wu, C.-H. Tung, D. O'Hare and T. Zhang, Layered Double Hydroxide Nanostructured Photocatalysts for Renewable Energy Production, *Adv. Energy Mater.*, 2016, **6**, 1501974.

90 Y. Zhao, Y. Zhao, G. I. N. Waterhouse, L. Zheng, X. Cao, F. Teng, L.-Z. Wu, C.-H. Tung, D. O'Hare and T. Zhang, Layered-Double-Hydroxide Nanosheets as Efficient Visible-Light-Driven Photocatalysts for Dinitrogen Fixation, *Adv. Mater.*, 2017, **29**, 1703828.